

OPTIMIZED SCHWARZ METHODS FOR MAXWELL'S EQUATIONS

V. DOLEAN*, M.J. GANDER† AND L. GERARDO-GIORDA‡

Abstract. Over the last two decades, classical Schwarz methods have been extended to systems of hyperbolic partial differential equations, and it was observed that the classical Schwarz method can be convergent even without overlap in certain cases. This is in strong contrast to the behavior of classical Schwarz methods applied to elliptic problems, for which overlap is essential for convergence. More recently, optimized Schwarz methods have been developed for elliptic partial differential equations. These methods use more effective transmission conditions between subdomains, and are also convergent without overlap for elliptic problems. Using a relation between Maxwell's equations and two scalar elliptic ones, we can explain why the classical Schwarz method applied to both the time harmonic and time discretized Maxwell's equations converges without overlap: the method is equivalent to a simple optimized Schwarz method for the corresponding scalar elliptic equation. Based on this insight, we show how to develop an entire hierarchy of optimized Schwarz methods for Maxwell's equations with greatly enhanced performance compared to the classical Schwarz method. We illustrate our findings with numerical results.

Key words. Schwarz algorithms, optimized transmission conditions, Maxwell's equations

AMS subject classifications. 65M55, 65F10, 65N22

1. Introduction. Schwarz algorithms experienced a second youth over the last decades, when distributed computers became more and more performant and available. Fundamental convergence results for the classical Schwarz methods were derived for many partial differential equations, and can now be found in several authoritative reviews, see [2, 38, 39], and books, see [32, 30, 37]. The Schwarz methods were also extended to systems of partial differential equations, such as the time harmonic Maxwell's equations, see [10, 6, 36], or to linear elasticity [16, 17], but much less is known about the behavior of the Schwarz methods applied to hyperbolic systems of equations. This is true in particular for the Euler equations, to which the Schwarz algorithm was first applied in [28, 29], where classical (characteristic) transmission conditions are used at the interfaces, or with more general transmission conditions in [5]. The analysis of such algorithms applied to systems proved to be very different from the scalar case, see [13, 14].

Over the last decade, a new class of Schwarz methods was developed for scalar partial differential equations, namely the optimized Schwarz methods. These methods use more effective transmission conditions than the classical Dirichlet conditions at the interfaces between subdomains. New transmission conditions were originally proposed for three different reasons: first, to obtain Schwarz algorithms that are convergent without overlap, see [25] for Robin conditions. The second motivation for changing the transmission conditions was to obtain a convergent Schwarz method for the Helmholtz equation, where the classical Schwarz algorithm is not convergent, even with overlap. As a remedy, approximate radiation conditions were introduced in [8, 10]. The third motivation was that the convergence rate of the classical Schwarz method is rather slow and very much dependent on the size of the overlap. In a

*UNIV. DE NICE SOPHIA-ANTIPOLIS, LABORATOIRE J.-A. DIEUDONNÉ, NICE, FRANCE. DOLEAN@UNICE.FR

†SECTION DE MATHÉMATIQUES, UNIVERSITÉ DE GENÈVE, CP 64, 1211 GENÈVE, MARTIN.GANDER@MATH.UNIGE.CH

‡DEPARTMENT. OF MATHEMATICS, UNIVERSITY OF TRENTO, ITALY. GERARDO@SCIENCE.UNITN.IT

short note on non-linear problems [23], Hagstrom et al. introduced Robin transmission conditions between subdomains and suggested nonlocal operators for best performance. In [3], these optimal, non-local transmission conditions were developed for advection-diffusion problems, with local approximations for small viscosity, and low order frequency approximations were proposed in [26, 7]. In [33], one can find low-frequency approximations of absorbing boundary conditions for Euler equations. Independently, at the algebraic level, generalized coupling conditions were introduced in [35, 34]. Optimized transmission conditions for the best performance of the Schwarz algorithm in a given class of local transmission conditions were first introduced for advection diffusion problems in [24], for the Helmholtz equation in [4, 22], and for Laplace's equation in [15]. For complete results and attainable performance for symmetric, positive definite problems, see [18], and for time dependant problems, see [21, 19].

The purpose of this paper is to design and analyze optimized Schwarz methods for Maxwell's equations in their fully general form; for the special case of a rot-rot formulation, see [1]. The paper is organized as follows: in Section 2, we present Maxwell's equations and a reformulation thereof with characteristic variables used in our analysis. In Section 3, we treat the case of time harmonic solutions. Following ideas presented in [11] for the Cauchy-Riemann equations, we show that the classical Schwarz method for Maxwell's equations, which uses characteristic Dirichlet transmission conditions between subdomains, is equivalent to a simple optimized Schwarz method applied to an equivalent Helmholtz equation. This explains why the classical Schwarz method in that case can be convergent even without overlap, and it allows us to develop an entire hierarchy of optimized Schwarz methods for Maxwell's equations with greatly enhanced performance. In Section 4, we show that all the arguments for the time harmonic case also apply to the case of time discretizations of Maxwell's equations. We then show in Section 5 numerical experiments in two and three spatial dimensions, both for the time harmonic and time discretized case, which illustrate the performance of the new optimized Schwarz methods for Maxwell's equations. In Section 6, we summarize our findings and conclude with an outlook on future research directions.

2. Maxwell's Equations. The hyperbolic system of Maxwell's equations describes the propagation of electromagnetic waves, and is given by

$$-\varepsilon \frac{\partial \mathbf{E}}{\partial t} + \operatorname{curl} \mathbf{H} = \mathbf{J}, \quad \mu \frac{\partial \mathbf{H}}{\partial t} + \operatorname{curl} \mathbf{E} = 0, \quad (2.1)$$

where $\mathbf{E} = (E_1, E_2, E_3)^T$ and $\mathbf{H} = (H_1, H_2, H_3)^T$ denote the electric and magnetic fields, respectively, ε is the *electric permittivity*, μ is the *magnetic permeability*, and \mathbf{J} is the applied current density. In the following, to simplify the notation, and without loss of generality, we normalize the parameters $\varepsilon = \mu = 1$, which corresponds to a scaling of time and the vector fields \mathbf{E} and \mathbf{H} , and we assume the applied current density to be divergence free, that is $\operatorname{div} \mathbf{J} = 0$. Denoting the vector of physical unknowns by

$$\mathbf{u} = (E_1, E_2, E_3, H_1, H_2, H_3)^T, \quad (2.2)$$

Maxwell's equations (2.1) can be rewritten in the form

$$\partial_t \mathbf{u} + G_x \partial_x \mathbf{u} + G_y \partial_y \mathbf{u} + G_z \partial_z \mathbf{u} = \mathbf{f}, \quad (2.3)$$

where the right hand side is given by $\mathbf{f} = (J_1, J_2, J_3, 0, 0, 0)^T$, and the coefficient matrices are of the form

$$G_l = \begin{bmatrix} & N_l \\ -N_l & \end{bmatrix}, \quad l = x, y, z,$$

where the 3×3 matrices N_l , $l = x, y, z$ are given by

$$N_x = \begin{bmatrix} 0 & 0 & 0 \\ 0 & 0 & 1 \\ 0 & -1 & 0 \end{bmatrix}, \quad N_y = \begin{bmatrix} 0 & 0 & -1 \\ 0 & 0 & 0 \\ 1 & 0 & 0 \end{bmatrix}, \quad N_z = \begin{bmatrix} 0 & 1 & 0 \\ -1 & 0 & 0 \\ 0 & 0 & 0 \end{bmatrix}.$$

For any unit vector $\mathbf{v} = (v_1, v_2, v_3)$, $\|\mathbf{v}\| = 1$, we can define the characteristic matrix of system (2.3) by

$$C(\mathbf{v}) = v_1 \begin{bmatrix} & N_x \\ -N_x & \end{bmatrix} + v_2 \begin{bmatrix} & N_y \\ -N_y & \end{bmatrix} + v_3 \begin{bmatrix} & N_z \\ -N_z & \end{bmatrix} = \begin{bmatrix} & N\mathbf{v} \\ -N\mathbf{v} & \end{bmatrix},$$

whose eigenvalues are the characteristic speed of propagation along the direction \mathbf{v} . By the structure of the matrices N_l , $l = x, y, z$, the matrix $C(\mathbf{v})$ is symmetric, and hence has real eigenvalues, which implies that the Maxwell's equations are hyperbolic, see [31].

If we consider Maxwell's equations (2.1) on the domain $\Omega = (0, 1) \times \mathbb{R}^2$, the characteristic matrix for the unit normal vector to the boundaries at $x = 0$ and $x = 1$, $\tilde{\mathbf{n}} = (1, 0, 0)$, is

$$C(\tilde{\mathbf{n}}) = \begin{pmatrix} & N_x \\ -N_x & \end{pmatrix}.$$

The eigenvalues of this matrix are

$$\lambda_{1,2} = -1, \quad \lambda_{3,4} = 0, \quad \lambda_{5,6} = 1,$$

and since the eigenvalues are not distinct, Maxwell's equations are not strictly hyperbolic, see [31]. The matrix of the left eigenvectors of $C(\tilde{\mathbf{n}})$ is given by

$$L = \begin{bmatrix} 0 & 0 & 0 & 1 & 0 & 0 \\ -1 & 0 & 0 & 0 & 1 & 0 \\ 0 & 1 & 0 & 0 & 0 & -1 \\ 0 & 0 & 1 & 0 & 0 & 0 \\ 0 & 1 & 0 & 0 & 0 & 1 \\ 1 & 0 & 0 & 0 & 1 & 0 \end{bmatrix},$$

which leads to the characteristic variables $\mathbf{w} = (w_1, w_2, w_3, w_4, w_5, w_6)^T$ associated with the direction $\tilde{\mathbf{n}}$, where

$$\begin{aligned} w_1 &= -\frac{1}{2}(E_2 - H_3), & w_2 &= \frac{1}{2}(E_3 + H_2), & w_3 &= H_1, \\ w_4 &= E_1, & w_5 &= \frac{1}{2}(E_2 + H_3), & w_6 &= -\frac{1}{2}(E_3 - H_2). \end{aligned} \quad (2.4)$$

In the following, we will denote by \mathbf{w}_+ , \mathbf{w}_0 and \mathbf{w}_- the characteristic variables associated with the positive, null, and negative eigenvalues respectively, that is

$$\mathbf{w}_- = (w_1, w_2)^T, \quad \mathbf{w}_0 = (w_3, w_4)^T, \quad \mathbf{w}_+ = (w_5, w_6)^T. \quad (2.5)$$

The boundary value problem in the characteristic variables, associated with Maxwell's equations (2.1) on the domain $\Omega = (0, 1) \times \mathbb{R}^2$,

$$\begin{cases} (\partial_t - \partial_x)w_1 + \frac{1}{2}\partial_z w_3 - \frac{1}{2}\partial_y w_4 &= \frac{1}{2}J_2, \\ (\partial_t - \partial_x)w_2 + \frac{1}{2}\partial_y w_3 + \frac{1}{2}\partial_z w_4 &= -\frac{1}{2}J_3, \\ \partial_t w_3 + \partial_z w_1 + \partial_y w_2 - \partial_z w_5 - \partial_y w_6 &= 0, \\ \partial_t w_4 - \partial_y w_1 + \partial_z w_2 - \partial_y w_5 + \partial_z w_6 &= -J_1, \\ (\partial_t + \partial_x)w_5 - \frac{1}{2}\partial_z w_3 - \frac{1}{2}\partial_y w_4 &= -\frac{1}{2}J_2, \\ (\partial_t + \partial_x)w_6 - \frac{1}{2}\partial_y w_3 + \frac{1}{2}\partial_z w_4 &= \frac{1}{2}J_3, \end{cases} \quad (2.6)$$

together with the characteristic boundary conditions

$$\mathbf{w}_+(0, y, z) = \mathbf{r}(y, z), \quad \mathbf{w}_-(1, y, z) = \mathbf{s}(y, z), \quad (y, z) \in \mathbb{R}^2, \quad (2.7)$$

and with the Silver-Müller radiation condition on the unbounded part of the domain

$$\lim_{r \rightarrow \infty} r(\mathbf{H} \times \mathbf{n} - \mathbf{E}) = 0 \quad (2.8)$$

where $r = |\mathbf{x}|$, $\mathbf{n} = \mathbf{x}/|\mathbf{x}|$, is well-posed, see [27].

3. The Case of Time Harmonic Solutions. As in the case of the second order wave equation, $\partial_{tt}u - \Delta u = f$, it is also suitable for Maxwell's equations to assume the wave to be periodic in time. In this case, the time derivative becomes an algebraic term, and only the spatial domain needs to be discretized for a numerical approximation of the solution. The harmonic solutions of Maxwell's equations are complex valued static vector fields \mathbf{E} and \mathbf{H} such that the dynamic fields

$$\mathcal{E}(\mathbf{x}, t) = \mathcal{R}e(\mathbf{E}(\mathbf{x}) \exp(i\omega t)), \quad \mathcal{H}(\mathbf{x}, t) = \mathcal{R}e(\mathbf{H}(\mathbf{x}) \exp(i\omega t))$$

satisfy Maxwell's equations (2.1). The positive real parameter ω is called the pulsation of the harmonic wave. The harmonic solutions \mathbf{E} and \mathbf{H} satisfy the time-harmonic equations

$$\text{curl } \mathbf{E} + i\omega \mathbf{H} = \mathbf{0}, \quad \text{curl } \mathbf{H} - i\omega \mathbf{E} = \mathbf{J}, \quad (3.1)$$

or, written in component form, and using the definition of \mathbf{u} in (2.2),

$$\begin{cases} -i\omega u_1 + \partial_y u_6 - \partial_z u_5 &= J_1, \\ -i\omega u_2 + \partial_z u_4 - \partial_x u_6 &= J_2, \\ -i\omega u_3 + \partial_x u_5 - \partial_y u_4 &= J_3, \\ i\omega u_4 + \partial_y u_3 - \partial_z u_2 &= 0, \\ i\omega u_5 + \partial_z u_1 - \partial_x u_3 &= 0, \\ i\omega u_6 + \partial_x u_2 - \partial_y u_1 &= 0. \end{cases} \quad (3.2)$$

The time-harmonic problem in characteristic variables is therefore

$$\begin{cases} (i\omega - \partial_x)w_1 + \frac{1}{2}\partial_z w_3 - \frac{1}{2}\partial_y w_4 &= \frac{1}{2}J_2, \\ (i\omega - \partial_x)w_2 + \frac{1}{2}\partial_y w_3 + \frac{1}{2}\partial_z w_4 &= -\frac{1}{2}J_3, \\ i\omega w_3 + \partial_z w_1 + \partial_y w_2 - \partial_z w_5 - \partial_y w_6 &= 0, \\ i\omega w_4 - \partial_y w_1 + \partial_z w_2 - \partial_y w_5 + \partial_z w_6 &= -J_1, \\ (i\omega + \partial_x)w_5 - \frac{1}{2}\partial_z w_3 - \frac{1}{2}\partial_y w_4 &= -\frac{1}{2}J_2, \\ (i\omega + \partial_x)w_6 - \frac{1}{2}\partial_y w_3 + \frac{1}{2}\partial_z w_4 &= \frac{1}{2}J_3. \end{cases} \quad (3.3)$$

3.1. Relation with Helmholtz Equations. We now derive the relation between the solution of the time harmonic Maxwell's equations (3.3) and the solution of a Helmholtz equation.

PROPOSITION 3.1. *Any component w_j , $j = 1, \dots, 6$, of the characteristic variables of Maxwell's equations (3.3) satisfies in the interior of $\Omega = (0, 1) \times \mathbb{R}^2$ the Helmholtz equation*

$$(\omega^2 + \Delta)w_j = f_j, \quad j = 1, 2, \dots, 6, \quad (3.4)$$

with right hand side given by

$$\begin{aligned} f_1 &= \frac{1}{2}(-(\partial_x + i\omega)J_2 + \partial_y J_1), & f_4 &= i\omega J_1, \\ f_2 &= \frac{1}{2}((\partial_x + i\omega)J_3 - \partial_z J_1), & f_5 &= \frac{1}{2}(-(\partial_x - i\omega)J_2 + \partial_y J_1), \\ f_3 &= -\partial_y J_3 + \partial_z J_2, & f_6 &= \frac{1}{2}((\partial_x - i\omega)J_3 - \partial_z J_1). \end{aligned} \quad (3.5)$$

Proof. From the last three equations in (3.2), we obtain u_j , $j = 4, 5, 6$ as functions of u_j , $j = 1, 2, 3$ only. Substituting these expressions for u_j , $j = 4, 5, 6$, into the first three equations in (3.2), we obtain a system for u_j , $j = 1, 2, 3$,

$$\begin{cases} \omega^2 u_1 + (\partial_{yy} + \partial_{zz})u_1 - \partial_{xy}u_2 - \partial_{xz}u_3 &= i\omega J_1, \\ \omega^2 u_2 + (\partial_{xx} + \partial_{zz})u_2 - \partial_{yz}u_3 - \partial_{xy}u_1 &= i\omega J_2, \\ \omega^2 u_3 + (\partial_{xx} + \partial_{yy})u_3 - \partial_{xz}u_1 - \partial_{yz}u_2 &= i\omega J_3. \end{cases} \quad (3.6)$$

We now eliminate the variable u_3 from the first two equations by differentiating the first one with respect to y and subtracting it from the second one differentiated with respect to x . We then eliminate u_3 also from the second and third equations by applying the operator $[\omega^2 + (\partial_{xx} + \partial_{yy})]$ to the second one and adding it to the third one differentiated with respect to y and z . After some simplifications, we obtain a new system for u_1 and u_2 ,

$$\begin{aligned} \partial_y((\omega^2 + \Delta)u_1) - \partial_x((\omega^2 + \Delta)u_2) &= i\omega[\partial_y J_1 - \partial_x J_2], \\ -\partial_{xy}((\omega^2 + \Delta)u_1) + (\omega^2 + \partial_{xx})((\omega^2 + \Delta)u_2) &= i\omega((\omega^2 + \partial_{xx} + \partial_{yy})J_2 + \partial_{yz}J_3). \end{aligned}$$

Applying ∂_x to the first equation and adding it to the second one, we finally obtain, after a division by ω^2 and using $\operatorname{div} \mathbf{J} = 0$,

$$(\omega^2 + \Delta)u_2 = i\omega J_2. \quad (3.7)$$

Similar manipulations in (3.6) allow us to reduce the system to a single equation in u_1 and u_3 as well, namely

$$(\omega^2 + \Delta)u_1 = i\omega J_1, \quad (\omega^2 + \Delta)u_3 = i\omega J_3. \quad (3.8)$$

On the other hand, we can eliminate from the first three equations in (3.2) the variables u_j , $j = 1, 2, 3$ as functions of u_j , $j = 4, 5, 6$. Proceeding as above, we obtain

$$(\omega^2 + \Delta)u_4 = -\partial_y J_3 + \partial_z J_2, \quad (\omega^2 + \Delta)u_5 = -\partial_z J_1 + \partial_x J_3, \quad (\omega^2 + \Delta)u_6 = -\partial_x J_2 + \partial_y J_1. \quad (3.9)$$

The result now follows by taking linear combinations of (3.7), (3.8) and (3.9). \square

In order to investigate the influence of boundary conditions on the relation, we consider now

$$(\omega^2 + \Delta)\tilde{w}_1 = \tilde{f}_1 \quad \text{in } \Omega, \quad (3.10)$$

together with the boundary conditions

$$(\partial_x - i\omega)\tilde{w}_1(0, y, z) = \tilde{r}_1(y, z), \quad \tilde{w}_1(1, y, z) = \tilde{s}_1(1, y, z), \quad (y, z) \in \mathbb{R}^2, \quad (3.11)$$

and with Sommerfeld radiation conditions on the unbounded part of the domain,

$$\lim_{r \rightarrow \infty} r \left(\frac{\partial \tilde{w}_1}{\partial r} - i\omega \tilde{w}_1 \right) = 0, \quad (3.12)$$

where $r = |\mathbf{x}|$. Its solution is very much related to the solution of the time harmonic Maxwell's equations (3.3) in $\Omega = (0, 1) \times \mathbb{R}^2$ with boundary conditions (2.7) and (2.8).

PROPOSITION 3.2. *Let \mathbf{w} be the solution of (3.3) with boundary conditions (2.7) and (2.8), and let \tilde{w}_1 be the solution of (3.10) with boundary conditions (3.11) and (3.12). If $\tilde{f}_1(x, y, z) = f_1(x, y, z)$ defined in (3.5), $\tilde{s}_1(y, z) = s_1(y, z)$, and*

$$\tilde{r}_1(y, z) = \Delta_{yz}^{-1} \left[(\partial_x + i\omega) [(\partial_{yy} - \partial_{zz})w_5 - 2\partial_{yz}w_6] + \partial_y (\partial_z J_3 + \partial_y J_2) \right] (0, y, z),$$

where Δ_{yz} denotes the Laplace operator in the y and z variables, then

$$\tilde{w}_1(x, y, z) = w_1(x, y, z) \quad \text{in } \bar{\Omega}.$$

Proof. Proposition 3.1 showed that the characteristic variable w_1 satisfies a Helmholtz equation in Ω with right hand side f_1 defined in (3.5). Since $f = \tilde{f}$ by assumption, the differential equations coincide and it suffices to verify the equivalence of the boundary conditions. Now, given a solution of Maxwell's equations with a Silver-Müller radiation condition, any of its components satisfies also a Sommerfeld radiation condition, see [27]. Therefore the same results holds for any characteristic variable by linear combinations. The Dirichlet condition at $(1, y, z)$ is identical, and thus there is nothing to show. For the condition at $(0, y, z)$, we consider the first two and the last two equations in (3.3), which form a 4×6 linear system. We can therefore determine the components of the solution w_j , $j = 1, \dots, 4$ as functions of w_5 and w_6 . For any $\mathbf{x} = (x, y, z) \in \bar{\Omega}$, it can be easily seen that we have

$$(\partial_x - i\omega)w_1 = \Delta_{yz}^{-1} [(\partial_x + i\omega)(\partial_{yy} - \partial_{zz})w_5 - 2\partial_{yz}(\partial_x + i\omega)w_6 + \partial_{yz}J_3 + \partial_{yy}J_2]. \quad (3.13)$$

In particular, relation (3.13) also holds at $(0, y, z)$, and hence w_1 satisfies (3.10) with boundary conditions (3.11), and the result follows by uniqueness. \square

REMARK 1. *Similar results can be obtained for any other propagating component of the characteristic variables, i.e. w_2 , w_5 , and w_6 , with boundary conditions given in (2.7) and with*

$$\begin{aligned} (\partial_x - i\omega)w_2 &= \Delta_{yz}^{-1} \left[(\partial_x + i\omega) [(\partial_{yy} - \partial_{zz})w_5 - 2\partial_{yz}w_6] + \partial_y (\partial_z J_3 + \partial_y J_2) \right], \quad \text{at } (0, y, z), \\ (\partial_x + i\omega)w_5 &= \Delta_{yz}^{-1} \left[(\partial_x - i\omega) [(\partial_{yy} - \partial_{zz})w_1 - 2\partial_{yz}w_2] + \partial_y (\partial_y J_3 + \partial_z J_2) \right], \quad \text{at } (1, y, z), \\ (\partial_x + i\omega)w_6 &= \Delta_{yz}^{-1} \left[(\partial_x - i\omega) [2\partial_{yz}w_1 + (\partial_{yy} - \partial_{zz})w_2] + \partial_y (\partial_y J_3 + \partial_z J_2) \right], \quad \text{at } (1, y, z). \end{aligned}$$

3.2. Classical Schwarz Algorithm for Maxwell's Equations. We consider now the problem (3.1) in $\Omega = (0, 1) \times \mathbb{R}^2$, with boundary conditions on $(0, y, z)$ and $(1, y, z)$ given by (2.7), and with the radiation conditions (2.8). We decompose the

domain into two subdomains $\Omega_1 := (0, b) \times \mathbb{R}^2$ and $\Omega_2 := (a, 1) \times \mathbb{R}^2$, and we denote the overlap by $L := b - a \geq 0$. We solve system (2.3) in both subdomains and we enforce on the subdomain interfaces the continuity of the incoming characteristic variables. There are two incoming characteristics on both interfaces. Hence, to have a well-posed problem, we have to impose two conditions on each subdomain. The classical Schwarz algorithm, using subscript to denote components, and superscript to denote the subdomain and the iteration count, is given by

$$\left\{ \begin{array}{l} i\omega \mathbf{u}^{1,n} + \sum_{l=x,y,z} G_l \partial_l \mathbf{u}^{1,n} = \mathbf{f} \text{ in } \Omega_1, \\ \mathbf{w}_+^{1,n}(0, y, z) = \mathbf{r}(y, z), \\ \mathbf{w}_-^{1,n}(b, y, z) = \mathbf{w}_-^{2,n-1}(b, y, z), \end{array} \right. \quad \left\{ \begin{array}{l} i\omega \mathbf{u}^{2,n} + \sum_{l=x,y,z} G_l \partial_l \mathbf{u}^{2,n} = \mathbf{f} \text{ in } \Omega_2, \\ \mathbf{w}_-^{2,n}(1, y, z) = \mathbf{s}(y, z), \\ \mathbf{w}_+^{2,n}(a, y, z) = \mathbf{w}_+^{1,n-1}(a, y, z), \end{array} \right. \quad (3.14)$$

where in the transmission conditions $(y, z) \in \mathbb{R}^2$. We are interested in the relation between algorithm (3.14) and the following simple optimized Schwarz algorithm for the Helmholtz equation,

$$\left\{ \begin{array}{l} (\omega^2 + \Delta) \tilde{w}_1^{1,n} = \tilde{f}_1 \text{ in } \Omega_1, \\ (\partial_x - i\omega) \tilde{w}_1^{1,n}(0, y, z) = \tilde{r}_1(y, z), \\ \tilde{w}_1^{1,n}(b, y, z) = \tilde{w}_1^{2,n-1}(b, y, z) \end{array} \right. \quad \left\{ \begin{array}{l} (\omega^2 + \Delta) \tilde{w}_1^{2,n} = \tilde{f}_1 \text{ in } \Omega_2, \\ \tilde{w}_1^{2,n}(1, y, z) = \tilde{s}_1(y, z), \\ (\partial_x - i\omega) \tilde{w}_1^{2,n}(a, y, z) = (\partial_x - i\omega) \tilde{w}_1^{1,n-1}(a, y, z). \end{array} \right. \quad (3.15)$$

PROPOSITION 3.3. *Let $w_1^{2,0}, w_2^{2,0}, w_5^{1,0}, w_6^{1,0}$ be given. If algorithm (3.15) is started with an initial guess $\tilde{w}_1^{1,0}$ and $\tilde{w}_1^{2,0}$ such that*

$$(\partial_x - i\omega) \tilde{w}_1^{1,0} = \Delta_{yz}^{-1} [(\partial_{yy} - \partial_{zz})(\partial_x + i\omega) w_5^{1,0} - 2\partial_{yz}(\partial_x - i\omega) w_6^{1,0} + \partial_{yz} J_3 + \partial_{yy} J_2],$$

and $\tilde{w}_1^{2,0} = w_1^{2,0}$, then for any $n \geq 1$, the first characteristic variable w_1 of the iterates of (3.14) and the iterates of (3.15) coincide, i.e.

$$w_1^{1,n} = \tilde{w}_1^{1,n}, \quad w_1^{2,n} = \tilde{w}_1^{2,n}.$$

Proof. The proof is by induction. Proposition 3.2 shows the result for $n = 1$. Assuming that the result holds at iteration $n - 1$, we obtain

$$(\partial_x - i\omega) \tilde{w}_1^{1,n-1} = \Delta_{yz}^{-1} [(\partial_x + i\omega) [(\partial_{yy} - \partial_{zz}) w_5^{1,n-1} - 2\partial_{yz} w_6^{1,n-1}] + \partial_y (\partial_z J_3 + \partial_y J_2)],$$

which holds in particular at (a, y, z) . By uniqueness, the boundary condition at $(1, y, z)$ implies then that $w_1^{2,n} = \tilde{w}_1^{2,n}$.

Similarly, we have $w_1^{1,n-1}(b, y, z) = \tilde{w}_1^{1,n-1}(b, y, z)$, and with the boundary condition at $(0, y, z)$ the result follows. \square

From Proposition 3.3, the classical Schwarz algorithm with Dirichlet transmission conditions applied to the time harmonic Maxwell's equations (3.2) is equivalent to a simple optimized Schwarz method for a related Helmholtz problem. This implies in particular the equivalent convergence behavior we show in the following proposition for an infinite domain $\Omega = \mathbb{R}^3$. In what follows, we denote by k_y and k_z the Fourier variables corresponding to a transform with respect to y and z , respectively.

PROPOSITION 3.4. *Let $\Omega = \mathbb{R}^3$, and consider Maxwell's equations (3.2) in Ω with the Silver-Müller radiation condition*

$$\lim_{r \rightarrow \infty} r (\mathbf{H} \times \mathbf{n} - \mathbf{E}) = 0 \quad (3.16)$$

where $r = |\mathbf{x}|$, $\mathbf{n} = \mathbf{x}/|\mathbf{x}|$. Let Ω be decomposed into $\Omega_1 := (-\infty, L) \times \mathbb{R}^2$ and $\Omega_2 := (0, +\infty) \times \mathbb{R}^2$, ($L \geq 0$). For any given initial guess $\mathbf{u}^{1,0} \in (L^2(\Omega_1))^6$, $\mathbf{u}^{2,0} \in (L^2(\Omega_2))^6$, the Schwarz algorithm (3.14) applied to system (3.2) converges for all Fourier modes such that $|\mathbf{k}|^2 := k_y^2 + k_z^2 \neq \omega^2$. The convergence factor is

$$R_{th} = \begin{cases} \left| \frac{\sqrt{\omega^2 - |\mathbf{k}|^2} - \omega}{\sqrt{\omega^2 - |\mathbf{k}|^2} + \omega} \right|, & \text{for } |\mathbf{k}|^2 < \omega^2, \\ e^{-\sqrt{|\mathbf{k}|^2 - \omega^2}L}, & \text{for } |\mathbf{k}|^2 > \omega^2. \end{cases} \quad (3.17)$$

Proof. Because of linearity, it suffices to analyze the convergence to the zero solution when the right hand side vanishes. Performing a Fourier transform of system (3.2) in the y and z direction, the first and the fourth equation provide an algebraic expression for \hat{u}_1 and \hat{u}_4 , which is in agreement with the fact that these are the characteristic variables associated with the null eigenvalue. Inserting these expressions into the remaining Fourier transformed equations, we obtain the first order system

$$\partial_x \begin{pmatrix} \hat{u}_2 \\ \hat{u}_3 \\ \hat{u}_5 \\ \hat{u}_6 \end{pmatrix} + \frac{i}{\omega} \begin{bmatrix} 0 & 0 & k_y k_z & \omega^2 - k_y^2 \\ 0 & 0 & k_z^2 - \omega^2 & -k_y k_z \\ -k_y k_z & k_y^2 - \omega^2 & 0 & 0 \\ \omega^2 - k_z^2 & k_y k_z & 0 & 0 \end{bmatrix} \begin{pmatrix} \hat{u}_2 \\ \hat{u}_3 \\ \hat{u}_5 \\ \hat{u}_6 \end{pmatrix} = \begin{pmatrix} 0 \\ 0 \\ 0 \\ 0 \end{pmatrix}. \quad (3.18)$$

The eigenvalues of the matrix in (3.18) and their corresponding eigenvectors are

$$\lambda_{1,2}^{TH} = -\sqrt{|\mathbf{k}|^2 - \omega^2}, \quad \mathbf{v}_1 = \begin{pmatrix} \frac{k_y k_z}{i\omega\sqrt{|\mathbf{k}|^2 - \omega^2}} \\ \frac{k_z^2 - \omega^2}{i\omega\sqrt{|\mathbf{k}|^2 - \omega^2}} \\ 1 \\ 0 \end{pmatrix}, \quad \mathbf{v}_2 = \begin{pmatrix} \frac{\omega^2 - k_y^2}{i\omega\sqrt{|\mathbf{k}|^2 - \omega^2}} \\ \frac{k_y k_z}{i\omega\sqrt{|\mathbf{k}|^2 - \omega^2}} \\ 0 \\ 1 \end{pmatrix}, \quad (3.19)$$

and

$$\lambda_{3,4}^{TH} = \sqrt{|\mathbf{k}|^2 - \omega^2}, \quad \mathbf{v}_3 = \begin{pmatrix} -\frac{k_y k_z}{i\omega\sqrt{|\mathbf{k}|^2 - \omega^2}} \\ \frac{\omega^2 - k_z^2}{i\omega\sqrt{|\mathbf{k}|^2 - \omega^2}} \\ 1 \\ 0 \end{pmatrix}, \quad \mathbf{v}_4 = \begin{pmatrix} \frac{k_y^2 - \omega^2}{i\omega\sqrt{|\mathbf{k}|^2 - \omega^2}} \\ \frac{k_y k_z}{i\omega\sqrt{|\mathbf{k}|^2 - \omega^2}} \\ 0 \\ 1 \end{pmatrix}. \quad (3.20)$$

Because of the radiation condition, the solutions \mathbf{u}^l of system (3.18) in Ω_l , $l = 1, 2$, are given by

$$\mathbf{u}^1 = (\alpha_1 \mathbf{v}_1 + \alpha_2 \mathbf{v}_2) e^{\sqrt{|\mathbf{k}|^2 - \omega^2}(x-L)}, \quad \mathbf{u}^2 = (\beta_1 \mathbf{v}_3 + \beta_2 \mathbf{v}_4) e^{-\sqrt{|\mathbf{k}|^2 - \omega^2}x}, \quad (3.21)$$

where the coefficients α_j and β_j ($j = 1, 2$) are uniquely determined by the transmission conditions. At the n -th step of the Schwarz algorithm, the coefficients $\boldsymbol{\alpha} = (\alpha_1, \alpha_2)$ and $\boldsymbol{\beta} = (\beta_1, \beta_2)$ satisfy the system

$$\boldsymbol{\alpha}^n = A_1^{-1} A_2 e^{-\sqrt{|\mathbf{k}|^2 - \omega^2}L} \boldsymbol{\beta}^{n-1}, \quad \boldsymbol{\beta}^n = B_1^{-1} B_2 e^{-\sqrt{|\mathbf{k}|^2 - \omega^2}L} \boldsymbol{\alpha}^{n-1},$$

where the matrices in the iteration are given by

$$A_1 = \begin{bmatrix} -k_y k_z & k_y^2 - \omega^2 + i\omega\lambda \\ k_z^2 - \omega^2 + i\omega\lambda & -k_y k_z \end{bmatrix}, \quad A_2 = \begin{bmatrix} k_y k_z & -(k_y^2 - \omega^2 - i\omega\lambda) \\ -(k_z^2 - \omega^2 - i\omega\lambda) & k_y k_z \end{bmatrix}, \quad (3.22)$$

and where $B_l = A_l, l = 1, 2$, and we have set $\lambda := \sqrt{|\mathbf{k}|^2 - \omega^2}$. A complete iteration over two steps of the Schwarz algorithm leads then to

$$\boldsymbol{\alpha}^{n+1} = A_1^{-1} A_2 B_1^{-1} B_2 e^{-2\lambda L} \boldsymbol{\alpha}^{n-1}, \quad \boldsymbol{\beta}^{n+1} = B_1^{-1} B_2 A_1^{-1} A_2 e^{-2\lambda L} \boldsymbol{\beta}^{n-1},$$

and we obtain

$$A_1^{-1} A_2 B_1^{-1} B_2 = B_1^{-1} B_2 A_1^{-1} A_2 = \left(\frac{|\mathbf{k}|^2}{(\lambda + i\omega)^2} \right)^2 Id.$$

Now by the definition of λ , we have $|\mathbf{k}|^2 = (\lambda - i\omega)(\lambda + i\omega)$, and thus the convergence factor of the algorithm is

$$\rho(|\mathbf{k}|) = \left| \frac{\sqrt{|\mathbf{k}|^2 - \omega^2} - i\omega}{\sqrt{|\mathbf{k}|^2 - \omega^2} + i\omega} e^{-\sqrt{|\mathbf{k}|^2 - \omega^2} L} \right|.$$

Separating the two cases $|\mathbf{k}|^2 < \omega^2$ and $|\mathbf{k}|^2 > \omega^2$ then concludes the proof. \square

Note that for $|\mathbf{k}|^2 = \omega^2$, the convergence factor equals 1, independently of the overlap, which indicates that the algorithm is not convergent in general when used in the iterative form described here. This precise result was also observed for the equivalent optimized Schwarz method applied to the Helmholtz equation, see [22]. In practice, Schwarz methods are however often used as preconditioners for Krylov methods, which can handle such situations.

We also see from the convergence factor (3.17) that the overlap is necessary for the convergence of the evanescent modes, $|\mathbf{k}|^2 > \omega^2$. Without overlap, $L = 0$, we have $\rho(|\mathbf{k}|) < 1$ only for the propagative modes, $|\mathbf{k}|^2 < \omega^2$, and $\rho(|\mathbf{k}|) = 1$ when $|\mathbf{k}|^2 \geq \omega^2$. In the time-harmonic case, the classical Schwarz algorithm without overlap is thus convergent only for propagative modes, and corresponds to the algorithm proposed by Desprès *et al.* in [9] for the Helmholtz equation.

3.3. Transparent Boundary Conditions. To design optimized Schwarz algorithms for Maxwell's equations, we derive now transparent boundary conditions for those equations. We consider the time harmonic Maxwell's equations (3.2) on the domain $\Omega = (0, 1) \times \mathbb{R}^2$, with right hand side \mathbf{J} compactly supported in Ω , together with the boundary conditions

$$(\mathbf{w}_+ + \mathcal{S}_1 \mathbf{w}_-)(0, y, z) = 0, \quad (\mathbf{w}_- + \mathcal{S}_2 \mathbf{w}_+)(1, y, z) = 0, \quad (y, z) \in \mathbb{R}^2, \quad (3.23)$$

where \mathbf{w}_- and \mathbf{w}_+ are defined in (2.5), and the operators $\mathcal{S}_l, l = 1, 2$, are general, pseudo-differential operators acting in the y and z directions.

LEMMA 3.5. *If the operators $\mathcal{S}_l, l = 1, 2$ have the Fourier symbol*

$$\mathcal{F}(\mathcal{S}_l) = \frac{1}{(\sqrt{|\mathbf{k}|^2 - \omega^2} + i\omega)^2} \begin{bmatrix} k_y^2 - k_z^2 & -2k_y k_z \\ -2k_y k_z & k_z^2 - k_y^2 \end{bmatrix}, \quad j = 1, 2, \quad (3.24)$$

then the solution of Maxwell's equations (3.2) in Ω with boundary conditions (3.23) coincides with the restriction on Ω of the solution of Maxwell's equations (3.2) on \mathbb{R}^3 .

Proof. We show that the difference \mathbf{e} between the solution of the global problem and the solution of the restricted problem vanishes. This difference satisfies in Ω the homogeneous counterpart of (3.2) with homogeneous boundary conditions (3.23), and we obtain after a Fourier transform in y and z

$$\hat{\mathbf{e}} = (\alpha_1 \mathbf{v}_1 + \alpha_2 \mathbf{v}_2) e^{\sqrt{|\mathbf{k}|^2 - \omega^2} x} + (\alpha_3 \mathbf{v}_3 + \alpha_4 \mathbf{v}_4) e^{-\sqrt{|\mathbf{k}|^2 - \omega^2} x},$$

where the vectors \mathbf{v}_j , $j = 1, \dots, 4$, are defined in (3.19) and (3.20). Using the boundary condition (3.23) at $(0, y, z)$, we obtain that the coefficients α_j , $j = 3, 4$, satisfy the system of equations

$$\begin{bmatrix} -k_y k_z & k_y^2 - \omega^2 + i\omega\sqrt{|\mathbf{k}|^2 - \omega^2} \\ k_z^2 - \omega^2 + i\omega\sqrt{|\mathbf{k}|^2 - \omega^2} & -k_y k_z \end{bmatrix} \begin{bmatrix} \alpha_3 \\ \alpha_4 \end{bmatrix} = \begin{bmatrix} 0 \\ 0 \end{bmatrix},$$

which implies $\alpha_3 = \alpha_4 = 0$. Now using the boundary condition at $(1, y, z)$, we obtain for the coefficients α_j , $j = 1, 2$, the same system of equations as for α_j , $j = 3, 4$, which implies $\alpha_1 = \alpha_2 = 0$. Thus $\hat{\mathbf{e}} = \mathbf{0}$, which concludes the proof. \square

REMARK 2. *As in the case of the Cauchy-Riemann equations, see [11], the symbols in (3.24) can be written in several, mathematically equivalent forms,*

$$\mathcal{F}(\mathcal{S}_l) = \frac{1}{(\sqrt{|\mathbf{k}|^2 - \omega^2} + i\omega)^2} M = \frac{1}{|\mathbf{k}|^2} \frac{\sqrt{|\mathbf{k}|^2 - \omega^2} - i\omega}{\sqrt{|\mathbf{k}|^2 - \omega^2} + i\omega} M = (\sqrt{|\mathbf{k}|^2 - \omega^2} - i\omega)^2 M^{-1},$$

where $M = \begin{bmatrix} k_y^2 - k_z^2 & -2k_y k_z \\ -2k_y k_z & k_z^2 - k_y^2 \end{bmatrix}$, which motivate different approximations of the transparent conditions in the context of optimized Schwarz methods. The first form contains a local and a non-local term, since multiplication with the matrix M corresponds to second order derivatives in y and z , which are local operations, whereas the term containing the square-root of $|\mathbf{k}|^2$ represents a non-local operation. The last form contains two non-local operations, since the inversion of the matrix M corresponds to an integration. This integration can however be passed to the other side of the transmission conditions by multiplication with the matrix M from the right. The second form contains two non-local terms and a local one.

Similarly, we can consider the associated Helmholtz equation (3.4) in $\Omega = (0, 1) \times \mathbb{R}^2$, with right hand side compactly supported in Ω , and with boundary conditions

$$(\partial_x - \tilde{\mathcal{S}}_1)\mathbf{u}(0, y, z) = 0, \quad (\partial_x + \tilde{\mathcal{S}}_2)\mathbf{u}(1, y, z) = 0, \quad (y, z) \in \mathbb{R}^2, \quad (3.25)$$

where $\tilde{\mathcal{S}}_j$ ($j = 1, 2$) are general, pseudo-differential operators acting in the y and z directions.

LEMMA 3.6. *If the operators $\tilde{\mathcal{S}}_l$ ($l = 1, 2$) have the Fourier symbol*

$$\tilde{\sigma}_l = \mathcal{F}(\tilde{\mathcal{S}}_l) = \sqrt{|\mathbf{k}|^2 - \omega^2} \quad (3.26)$$

then the solution of (3.4) in Ω with boundary conditions (3.25) coincides with the restriction to Ω of the solution of the Helmholtz equation (3.4) on \mathbb{R}^3 with Sommerfeld radiation condition (3.12).

Proof. The proof follows along the same lines as in the previous Lemma. Performing a Fourier transform in the y and z directions, the symbol of the difference between the solution of the global problem and the solution of the restricted one, denoted by $\tilde{\mathbf{e}}$, is given by

$$\tilde{\mathbf{e}} = \alpha e^{\sqrt{|\mathbf{k}|^2 - \omega^2}} + \beta e^{-\sqrt{|\mathbf{k}|^2 - \omega^2}}.$$

The boundary condition at $(0, y, z)$ implies then that $\alpha = 0$, whereas the boundary condition at $(1, y, z)$ implies that $\beta = 0$, which concludes the proof. \square

3.4. Optimized Schwarz Algorithms for Maxwell's Equations. The transparent operators \mathcal{S}_l , $l = 1, 2$, introduced in Subsection 3.3, are important in the development of optimized Schwarz methods. They lead to the best possible performance of the method, as we will show in Remark 3. The transparent operators are however unfortunately non-local operators, and hence difficult to use in practice. In optimized Schwarz methods, they are therefore approximated to obtain practical methods. If one is willing to use second order transmission conditions, then the only parts of the symbols in (3.24) that need to be approximated are the multiplications by $(\sqrt{|\mathbf{k}|^2 - \omega^2} + i\omega)^{-2}$, because the entries of the matrices are polynomials in the Fourier variables, which correspond to derivatives in the y and z direction.

We now introduce a Schwarz algorithm for Maxwell's equations (3.2) with more general transmission conditions, which are for Ω_1 given by

$$[(\mathbf{w}_- + \mathcal{S}_1 \mathbf{w}_+)(L, y, z)]^{1,n} = [(\mathbf{w}_- + \mathcal{S}_1 \mathbf{w}_+)(L, y, z)]^{2,n-1}, \quad (y, z) \in \mathbb{R}^2, \quad (3.27)$$

and for Ω_2 by

$$[(\mathbf{w}_+ + \mathcal{S}_2 \mathbf{w}_-)(0, y, z)]^{2,n} = [(\mathbf{w}_+ + \mathcal{S}_2 \mathbf{w}_-)(0, y, z)]^{1,n-1}, \quad (y, z) \in \mathbb{R}^2. \quad (3.28)$$

PROPOSITION 3.7. **a)** If the operators \mathcal{S}_1 and \mathcal{S}_2 have the Fourier symbol

$$\sigma_l := \mathcal{F}(\mathcal{S}_l) = \gamma_l \begin{bmatrix} k_y^2 - k_z^2 & -2k_y k_z \\ -2k_y k_z & k_z^2 - k_y^2 \end{bmatrix}, \quad \gamma_l \in \mathbb{C}(k_z, k_y) \quad (l = 1, 2), \quad (3.29)$$

then the convergence factor of the Schwarz algorithm with transmission conditions (3.27)-(3.28) is

$$\rho(\omega, L, |\mathbf{k}|, \gamma_1, \gamma_2) = \left| \frac{(\sqrt{|\mathbf{k}|^2 - \omega^2} - i\omega)^2}{(\sqrt{|\mathbf{k}|^2 - \omega^2} + i\omega)^2} \frac{1 - \gamma_1(\sqrt{|\mathbf{k}|^2 - \omega^2} + i\omega)^2}{1 - \gamma_1(\sqrt{|\mathbf{k}|^2 - \omega^2} - i\omega)^2} \frac{1 - \gamma_2(\sqrt{|\mathbf{k}|^2 - \omega^2} + i\omega)^2}{1 - \gamma_2(\sqrt{|\mathbf{k}|^2 - \omega^2} - i\omega)^2} e^{-2\sqrt{|\mathbf{k}|^2 - \omega^2}L} \right|^{\frac{1}{2}}. \quad (3.30)$$

b) If the operators \mathcal{S}_1 and \mathcal{S}_2 have the Fourier symbol

$$\sigma_l := \mathcal{F}(\mathcal{S}_l) = \delta_l \begin{bmatrix} k_y^2 - k_z^2 & -2k_y k_z \\ -2k_y k_z & k_z^2 - k_y^2 \end{bmatrix}^{-1}, \quad \gamma_l \in \mathbb{C}(k_z, k_y) \quad (l = 1, 2), \quad (3.31)$$

then the convergence factor of the Schwarz algorithm with transmission conditions (3.27)-(3.28) is

$$\rho(\omega, L, |\mathbf{k}|, \delta_1, \delta_2) = \left| \frac{(\sqrt{|\mathbf{k}|^2 - \omega^2} + i\omega)^2}{(\sqrt{|\mathbf{k}|^2 - \omega^2} - i\omega)^2} \frac{\delta_1 - (\sqrt{|\mathbf{k}|^2 - \omega^2} - i\omega)^2}{\delta_1 - (\sqrt{|\mathbf{k}|^2 - \omega^2} + i\omega)^2} \frac{\delta_2 - (\sqrt{|\mathbf{k}|^2 - \omega^2} - i\omega)^2}{\delta_2 - (\sqrt{|\mathbf{k}|^2 - \omega^2} + i\omega)^2} e^{-2\sqrt{|\mathbf{k}|^2 - \omega^2}L} \right|^{\frac{1}{2}}. \quad (3.32)$$

c) If the operator \mathcal{S}_1 has the Fourier symbol (3.29) and \mathcal{S}_2 has the Fourier symbol (3.31), then the convergence factor of the Schwarz algorithm with transmission conditions (3.27)-(3.28) is

$$\rho(\omega, L, |\mathbf{k}|, \gamma_1, \delta_2) = \left| \frac{1 - \gamma_1(\sqrt{|\mathbf{k}|^2 - \omega^2} + i\omega)^2}{1 - \gamma_1(\sqrt{|\mathbf{k}|^2 - \omega^2} - i\omega)^2} \frac{\delta_2 - (\sqrt{|\mathbf{k}|^2 - \omega^2} - i\omega)^2}{\delta_2 - (\sqrt{|\mathbf{k}|^2 - \omega^2} + i\omega)^2} e^{-2\sqrt{|\mathbf{k}|^2 - \omega^2}L} \right|^{1/2}. \quad (3.33)$$

Proof. The convergence result is again based on Fourier analysis, as in Section 3.2. At the n -th step of the Schwarz algorithm, the coefficients $\boldsymbol{\alpha}^n = (\alpha_1^n, \alpha_2^n)$ and $\boldsymbol{\beta} = (\beta_1, \beta_2)$ in (3.21) satisfy

$$\boldsymbol{\alpha}^n = \bar{A}_1^{-1} \bar{A}_2 e^{-\lambda L} \boldsymbol{\beta}^{n-1}, \quad \boldsymbol{\beta}^n = \bar{B}_1^{-1} \bar{B}_2 e^{-\lambda L} \boldsymbol{\alpha}^{n-1}, \quad (3.34)$$

where $\lambda = \sqrt{|\mathbf{k}|^2 - \omega^2}$, and the matrices \bar{A}_l and \bar{B}_l , $l = 1, 2$, are given by

$$\bar{A}_1 = A_1 + \sigma_1 A_2, \quad \bar{A}_2 = A_2 + \sigma_1 A_1, \quad \bar{B}_1 = A_1 + \sigma_2 A_2, \quad \bar{B}_2 = A_2 + \sigma_2 A_1,$$

with A_l , $l = 1, 2$, defined in (3.22). A complete double iteration of the Schwarz algorithm leads therefore to

$$\boldsymbol{\alpha}^{n+1} = \bar{A}_1^{-1} \bar{A}_2 \bar{B}_1^{-1} \bar{B}_2 e^{-2\lambda L} \boldsymbol{\alpha}^{n-1}, \quad \boldsymbol{\beta}^{n+1} = \bar{B}_1^{-1} \bar{B}_2 \bar{A}_1^{-1} \bar{A}_2 e^{-2\lambda L} \boldsymbol{\beta}^{n-1}.$$

a) In this case we obtain the iteration matrix

$$\bar{A}_1^{-1} \bar{A}_2 \bar{B}_1^{-1} \bar{B}_2 = \bar{B}_1^{-1} \bar{B}_2 \bar{A}_1^{-1} \bar{A}_2 = \left(\frac{|\mathbf{k}|^2}{(\lambda + i\omega)^2} \right)^2 \frac{(1 - \gamma_1(\lambda + i\omega)^2)(1 - \gamma_2(\lambda + i\omega)^2)}{(1 - \gamma_1(\lambda - i\omega)^2)(1 - \gamma_2(\lambda - i\omega)^2)} Id,$$

and since $|\mathbf{k}|^2 = (\lambda - i\omega)(\lambda + i\omega)$, the result follows.

b) In this case the iteration matrix is

$$\bar{A}_1^{-1} \bar{A}_2 \bar{B}_1^{-1} \bar{B}_2 = \bar{B}_1^{-1} \bar{B}_2 \bar{A}_1^{-1} \bar{A}_2 = \left(\frac{|\mathbf{k}|^2}{(\lambda - i\omega)^2} \right)^2 \frac{(\delta_1 - (\lambda - i\omega)^2)(\delta_2 - (\lambda - i\omega)^2)}{(\delta_1 - (\lambda + i\omega)^2)(\delta_2 - (\lambda + i\omega)^2)} Id,$$

and the result follows as in the first case.

c) The conclusion follows as in the first two cases. \square

REMARK 3. From (3.30), we see that the choice $\gamma_1 = \gamma_2 = 1/(\sqrt{|\mathbf{k}|^2 - \omega^2} + i\omega)^2$ is optimal, since then $\rho_{th}(|\mathbf{k}|) \equiv 0$, for all frequencies $|\mathbf{k}|$. With this choice of γ_1 and γ_2 , the matrices \bar{A}_2 and \bar{B}_2 actually vanish.

3.5. Relation to a Schwarz Algorithm for a Scalar Equation. We present here several particular choices of the transmission operator \mathcal{S}_l with Fourier symbol σ_l ($l = 1, 2$) in the transmission conditions (3.27) and (3.28).

Case 1: taking $\gamma_1 = \gamma_2 = 0$ in (3.29), which amounts to enforce the classical characteristic Dirichlet transmission conditions, the convergence factor is

$$\rho_1(\omega, L, |\mathbf{k}|) = \left| \left(\frac{\sqrt{|\mathbf{k}|^2 - \omega^2} - i\omega}{\sqrt{|\mathbf{k}|^2 - \omega^2} + i\omega} \right)^2 e^{-2\sqrt{|\mathbf{k}|^2 - \omega^2}L} \right|^{\frac{1}{2}}.$$

In the non-overlapping case, $L = 0$, this choice ensures convergence only for propagative modes, and corresponds to the Taylor transmission conditions of order zero proposed in [9] for the Helmholtz equation.

Case 2: taking $\gamma_1 = \gamma_2 = \frac{1}{|\mathbf{k}|^2} \frac{s - i\omega}{s + i\omega}$ in (3.29) or $\gamma_1 = \frac{1}{|\mathbf{k}|^2 - 2\omega^2 + 2i\omega s}$ in (3.29) and $\delta_2 = |\mathbf{k}|^2 - 2\omega^2 - 2i\omega s$ in (3.31) with $s \in \mathbb{C}$, the convergence factor is

$$\rho_2(\omega, L, |\mathbf{k}|, s) = \left| \left(\frac{\sqrt{|\mathbf{k}|^2 - \omega^2} - s}{\sqrt{|\mathbf{k}|^2 - \omega^2} + s} \right)^2 e^{-2\sqrt{|\mathbf{k}|^2 - \omega^2}L} \right|^{\frac{1}{2}}.$$

Case 3: taking $\gamma_1 = \gamma_2 = \frac{1}{|\mathbf{k}|^2 - 2\omega^2 + 2i\omega s}$ in (3.29) with $s \in \mathbb{C}$, the convergence factor is

$$\rho_3(\omega, L, |\mathbf{k}|, s) = \left| \frac{\sqrt{|\mathbf{k}|^2 - \omega^2} - i\omega}{\sqrt{|\mathbf{k}|^2 - \omega^2} + i\omega} \right| \rho_2(\omega, L, |\mathbf{k}|, s) \leq \rho_2(\omega, L, |\mathbf{k}|, s).$$

Case 4: taking $\gamma_l = \frac{1}{|\mathbf{k}|^2} \frac{s_l - i\omega}{s_l + i\omega}$, $l = 1, 2$ in (3.29) or $\gamma_1 = \frac{1}{|\mathbf{k}|^2 - 2\omega^2 + 2i\omega s_1}$ in (3.29) and $\delta_2 = |\mathbf{k}|^2 - 2\omega^2 - 2i\omega s_2$ in (3.31) with $s_l \in \mathbb{C}$, $l = 1, 2$, the convergence factor is

$$\rho_4(\omega, L, |\mathbf{k}|, s_1, s_2) = \left| \frac{\sqrt{|\mathbf{k}|^2 - \omega^2} - s_1}{\sqrt{|\mathbf{k}|^2 - \omega^2} + s_1} \frac{\sqrt{|\mathbf{k}|^2 - \omega^2} - s_2}{\sqrt{|\mathbf{k}|^2 - \omega^2} + s_2} e^{-2\sqrt{|\mathbf{k}|^2 - \omega^2} L} \right|^{\frac{1}{2}}.$$

Case 5: taking $\gamma_l = \frac{1}{|\mathbf{k}|^2 - 2\omega^2 + 2i\omega s_l}$ in (3.29) with $s_l \in \mathbb{C}$, $l = 1, 2$, the convergence factor is

$$\rho_5(\omega, L, |\mathbf{k}|, s_1, s_2) = \left| \frac{\sqrt{|\mathbf{k}|^2 - \omega^2} - i\omega}{\sqrt{|\mathbf{k}|^2 - \omega^2} + i\omega} \right| \rho_4(\omega, L, |\mathbf{k}|, s_1, s_2) \leq \rho_4(\omega, L, |\mathbf{k}|, s_1, s_2).$$

Except for Case 1, all cases use second order transmission conditions, even though we use only a zeroth order approximation of the non-local operator $\sqrt{|\mathbf{k}|^2 - \omega^2}$. In Case 2 and Case 4, the convergence factor is the same as the one obtained for optimized Schwarz methods for the Helmholtz equation in [22]. In the cases with parameters, the best choice for the parameters is in general the one that minimizes the convergence factor for all $|\mathbf{k}| \in K$, where K denotes the set of relevant numerical frequencies. One therefore needs to solve the min-max problems

$$\min_{s \in \mathbb{C}} \max_{|\mathbf{k}| \in K} \rho_j(\omega, L, |\mathbf{k}|, s), \quad j = 2, 3, \quad \min_{s_1, s_2 \in \mathbb{C}} \max_{|\mathbf{k}| \in K} \rho_j(\omega, L, |\mathbf{k}|, s_1, s_2) \quad j = 4, 5. \quad (3.35)$$

We can choose $K = [(k_{\min}, k_-) \cup (k_+, k_{\max})]^2$, where k_{\min} denotes the smallest frequency relevant to the subdomain, $k_{\max} = \frac{C}{h}$ denotes the largest frequency supported by the numerical grid with mesh size h , and k_{\pm} are parameters to be chosen to exclude the resonance frequencies. If for example the domain Ω is a rectilinear conductor with homogeneous Dirichlet conditions on the lateral surface, the solution is the sum of the transverse electric (TE) and transverse magnetic (TM) fields. If the transverse section of the conductor is a rectangle with sides of length a and b , the TE and TM fields can be expanded in a Fourier series with the harmonics $\sin(\frac{n\pi y}{a}) \sin(\frac{m\pi z}{b})$, where the relevant frequencies are $|\mathbf{k}| = \pi \sqrt{\frac{m^2}{a^2} + \frac{n^2}{b^2}}$, $m, n \in \mathbb{N}^+$. The lowest one is therefore $k_{\min} = \pi \sqrt{\frac{1}{a^2} + \frac{1}{b^2}}$, and if the mesh size h satisfies $h = \frac{a}{N} = \frac{b}{M}$, where N and M are the number of grid points in the y and z direction, then the highest frequency would be $k_{\max} = \frac{\sqrt{2}\pi}{h}$. The parameters k_{\pm} would correspond to the frequencies closest to ω , i.e. $k_- = \pi \sqrt{\frac{m_-^2}{a^2} + \frac{n_-^2}{b^2}}$ and $k_+ = \pi \sqrt{\frac{m_+^2}{a^2} + \frac{n_+^2}{b^2}}$, where $\pi \sqrt{\frac{m_-^2}{a^2} + \frac{n_-^2}{b^2}} < \omega < \pi \sqrt{\frac{m_+^2}{a^2} + \frac{n_+^2}{b^2}}$, but such precise estimates are not necessary if Krylov acceleration is used, see [22, 20].

Using the results in [20] for Case 2 and Case 4, which are identical to the Helmholtz case, and optimization techniques as in [20] for the other cases, we obtain asymptotic formulas for the optimized parameters, of the form $s = p(1 - i)$ and $s_l = p_l(1 - i)$, $l = 1, 2$, with p and p_l shown in Table 3.1.

4. The Case of Time Discretization. If we do not assume the wave to be periodic in time, the time domain also needs to be discretized. We consider a uniform time grid with time step Δt , and use a semi-implicit time integration scheme for the time derivative in (2.1) of the form

$$-\frac{\mathbf{E}^{n+1} - \mathbf{E}^n}{\Delta t} + \text{curl} \left(\frac{\mathbf{H}^{n+1} + \mathbf{H}^n}{2} \right) = \mathbf{J}, \quad \frac{\mathbf{H}^{n+1} - \mathbf{H}^n}{\Delta t} + \text{curl} \left(\frac{\mathbf{E}^{n+1} + \mathbf{E}^n}{2} \right) = \mathbf{0},$$

| Case | with overlap, $L = h$ | | without overlap, $L = 0$ | |
|------|---|---|---|---|
| | ρ | parameters | ρ | parameters |
| 1 | $1 - \sqrt{k_+ - \omega^2}h$ | none | 1 | none |
| 2 | $1 - 2C_\omega^{\frac{1}{6}}h^{\frac{1}{3}}$ | $p = \frac{C_\omega^{\frac{1}{3}}}{2 \cdot h^{\frac{2}{3}}}$ | $1 - \frac{\sqrt{2}C_\omega^{\frac{1}{4}}}{\sqrt{C}}\sqrt{h}$ | $p = \frac{\sqrt{C}C_\omega^{\frac{1}{4}}}{\sqrt{2}\sqrt{h}}$ |
| 3 | $1 - 2(k_+^2 - \omega^2)^{\frac{1}{6}}h^{\frac{1}{3}}$ | $p = \frac{(k_+^2 - \omega^2)^{\frac{1}{3}}}{2 \cdot h^{\frac{2}{3}}}$ | $1 - \frac{\sqrt{2}(k_+^2 - \omega^2)^{\frac{1}{4}}}{\sqrt{C}}\sqrt{h}$ | $p = \frac{\sqrt{C}(k_+^2 - \omega^2)^{\frac{1}{4}}}{\sqrt{2}\sqrt{h}}$ |
| 4 | $1 - 2^{\frac{2}{5}}C_\omega^{\frac{1}{10}}h^{\frac{1}{5}}$ | $\begin{cases} p_1 = \frac{C_\omega^{\frac{2}{5}}}{2^{\frac{2}{5}} \cdot h^{\frac{4}{5}}}, \\ p_2 = \frac{C_\omega^{\frac{3}{5}}}{2^{\frac{3}{5}} \cdot h^{\frac{4}{5}}} \end{cases}$ | $1 - \frac{C_\omega^{\frac{1}{8}}}{C^{\frac{1}{4}}}h^{\frac{1}{4}}$ | $\begin{cases} p_1 = \frac{C_\omega^{\frac{3}{8}} \cdot C^{\frac{1}{4}}}{2 \cdot h^{\frac{3}{4}}}, \\ p_2 = \frac{C_\omega^{\frac{5}{8}} \cdot C^{\frac{3}{4}}}{h^{\frac{3}{4}}} \end{cases}$ |
| 5 | $1 - 2^{\frac{2}{5}}(k_+^2 - \omega^2)^{\frac{1}{10}}h^{\frac{1}{5}}$ | $\begin{cases} p_1 = \frac{(k_+^2 - \omega^2)^{\frac{2}{5}}}{2^{\frac{2}{5}} \cdot h^{\frac{4}{5}}}, \\ p_2 = \frac{(k_+^2 - \omega^2)^{\frac{3}{5}}}{2^{\frac{3}{5}} \cdot h^{\frac{4}{5}}} \end{cases}$ | $1 - \frac{(k_+^2 - \omega^2)^{\frac{1}{8}}}{C^{\frac{1}{4}}}h^{\frac{1}{4}}$ | $\begin{cases} p_1 = \frac{(k_+^2 - \omega^2)^{\frac{3}{8}} \cdot C^{\frac{1}{4}}}{2 \cdot h^{\frac{3}{4}}}, \\ p_2 = \frac{(k_+^2 - \omega^2)^{\frac{5}{8}} \cdot C^{\frac{3}{4}}}{h^{\frac{3}{4}}} \end{cases}$ |

TABLE 3.1

Asymptotic convergence factor and optimal choice of the parameters in the transmission conditions for the five variants of the optimized Schwarz method applied to Maxwell's equations, when the mesh parameter h is small, and the maximum numerical frequency is estimated by $k_{\max} = \frac{C}{h}$, and where $C_\omega = \min(k_+^2 - \omega^2, \omega^2 - k_-^2)$.

where the mean value is introduced to ensure energy conservation, see [12]. With this time discretization, we have to solve at each time step the system

$$\begin{aligned} -\sqrt{\eta}E_1 + \partial_y H_3 - \partial_z H_2 &= \tilde{J}_1, & \sqrt{\eta}H_1 + \partial_y E_3 - \partial_z E_2 &= g_1, \\ -\sqrt{\eta}E_2 + \partial_z H_1 - \partial_x H_3 &= \tilde{J}_2, & \sqrt{\eta}H_2 + \partial_z E_1 - \partial_x E_3 &= g_2, \\ -\sqrt{\eta}E_3 + \partial_x H_2 - \partial_y H_1 &= \tilde{J}_3, & \sqrt{\eta}H_3 + \partial_x E_2 - \partial_y E_1 &= g_3, \end{aligned} \quad (4.1)$$

where we have set $(\mathbf{E}, \mathbf{H}) := (\mathbf{E}^{n+1}, \mathbf{H}^{n+1})$, $\sqrt{\eta} := \frac{2}{\Delta t}$, $\tilde{\mathbf{J}} := \mathbf{J} - \frac{2}{\Delta t}\mathbf{E}^n - \text{curl } \mathbf{H}^n$, $\mathbf{g} = \frac{2}{\Delta t}\mathbf{H}^n - \text{curl } \mathbf{E}^n$, and E_j and H_j denote the new fields at time step $n+1$. As in the time harmonic case, we have the equivalent of Proposition 3.1:

PROPOSITION 4.1. *Let \mathbf{u} be as defined in (2.2). At time step $n+1$, any component u_i of the solution of Maxwell's equations (4.1) satisfies the elliptic equation*

$$(\eta - \Delta)u_j = f_j, \quad (4.2)$$

where the right hand side depends on \mathbf{J} , η , and the solution at the previous time step, \mathbf{u}^n .

Proof. The result follows like in the time harmonic case. \square

In contrast to the time harmonic case however, (4.2) is a positive definite Helmholtz equation, which is much easier to solve numerically than the Helmholtz equation (3.4).

There is also an equivalence result including boundary conditions, as in Proposition 3.2, for which we omit the details here. Instead, we state directly the equivalent of Proposition 3.4, i.e a convergence result for the classical Schwarz algorithm applied to the time discretized Maxwell's equations.

PROPOSITION 4.2. *Let $\Omega = \mathbb{R}^3$, and consider Maxwell's equations (3.2) in Ω with the Silver-Müller radiation condition*

$$\lim_{r \rightarrow \infty} r(\mathbf{H} \times \mathbf{n} - \mathbf{E}) = 0 \quad (4.3)$$

where $r = |\mathbf{x}|$, $\mathbf{n} = \mathbf{x}/|\mathbf{x}|$. Let Ω be decomposed into $\Omega_1 := (-\infty, L) \times \mathbb{R}^2$ and $\Omega_2 := (0, +\infty) \times \mathbb{R}^2$, ($L \geq 0$). For any given initial guess $\mathbf{u}^{1,0} \in (L^2(\Omega_1))^6$, $\mathbf{u}^{2,0} \in$

| | with overlap, $L = h$ | | without overlap, $L = 0$ | |
|------|---|---|--|--|
| Case | ρ | parameters | ρ | parameters |
| 1 | $1 - 2^{\frac{3}{2}}\eta^{\frac{1}{4}}\sqrt{h}$ | none | $1 - 2\frac{\sqrt{\eta}}{C}h$ | none |
| 2 | $1 - 2^{\frac{13}{6}}\eta^{\frac{1}{6}}h^{\frac{1}{3}}$ | $p = \frac{2^{-\frac{1}{3}}\eta^{\frac{1}{3}}}{h^{\frac{1}{3}}}$ | $1 - \frac{4\eta^{\frac{1}{4}}\sqrt{h}}{\sqrt{C}}$ | $p = \frac{\sqrt{C}\eta^{\frac{1}{4}}}{\sqrt{h}}$ |
| 3 | $1 - 2^{\frac{7}{4}}\eta^{\frac{1}{8}}h^{\frac{1}{4}}$ | $p = \frac{\sqrt{2}\eta^{\frac{1}{4}}}{\sqrt{h}}$ | $1 - \frac{2^{\frac{5}{3}}\eta^{\frac{1}{6}}}{C^{\frac{1}{3}}}h^{\frac{1}{3}}$ | $p = \frac{2^{\frac{2}{3}}C^{\frac{2}{3}}\eta^{\frac{1}{6}}}{h^{\frac{2}{3}}}$ |
| 4 | $1 - 2^{\frac{4}{5}}\eta^{\frac{1}{10}}h^{\frac{1}{5}}$ | $p_1 = \frac{\eta^{\frac{1}{5}}}{2^{\frac{2}{5}}h^{\frac{4}{5}}}, p_2 = \frac{\eta^{\frac{2}{5}}}{16^{\frac{1}{5}}h^{\frac{1}{5}}}$ | $1 - \frac{\sqrt{2}\eta^{\frac{1}{8}}}{C^{\frac{1}{4}}}h^{\frac{1}{4}}$ | $p_1 = \frac{\sqrt{2}C^{\frac{3}{4}}\eta^{\frac{1}{8}}}{h^{\frac{3}{4}}}, p_2 = \frac{C^{\frac{1}{4}}\eta^{\frac{3}{8}}}{\sqrt{2}h^{\frac{1}{4}}}$ |
| 5 | $1 - 2^{\frac{7}{6}}\eta^{\frac{1}{12}}h^{\frac{1}{6}}$ | $p_1 = \frac{2^{\frac{2}{3}}\eta^{\frac{1}{3}}}{h^{\frac{1}{3}}}, p_2 = \frac{2^{\frac{1}{3}}\eta^{\frac{1}{6}}}{h^{\frac{2}{3}}}$ | $1 - \frac{2\eta^{\frac{1}{10}}}{C^{\frac{1}{5}}}h^{\frac{1}{5}}$ | $p_1 = \frac{2C^{\frac{4}{5}}\eta^{\frac{1}{10}}}{h^{\frac{4}{5}}}, p_2 = \frac{2C^{\frac{2}{5}}\eta^{\frac{3}{10}}}{h^{\frac{2}{5}}}$ |

TABLE 4.1

Asymptotic convergence factor and optimal choice of the parameters in the transmission conditions for the five variants of the optimized Schwarz method applied to the time domain Maxwell's equations, when the mesh parameter h is small, and the maximum numerical frequency is estimated by $k_{\max} = \frac{C}{h}$.

$(L^2(\Omega_2))^6$, the Schwarz algorithm

$$\begin{cases} \sqrt{\eta}\mathbf{u}^{1,n} + \sum_{l=x,y,z} G_l \partial_l \mathbf{u}^{1,n} = \mathbf{f} \text{ in } \Omega_1, \\ \mathbf{w}_-^{1,n}(b, y, z) = \mathbf{w}_-^{2,n-1}(b, y, z), \end{cases} \quad \begin{cases} \sqrt{\eta}\mathbf{u}^{2,n} + \sum_{l=x,y,z} \mathbf{G}_l \partial_l \mathbf{u}^{2,n} = \mathbf{f} \text{ in } \Omega_2, \\ \mathbf{w}_+^{2,n}(a, y, z) = \mathbf{w}_+^{1,n-1}(a, y, z), \end{cases} \quad (4.4)$$

converges for all Fourier modes to the solution of (4.1),

$$\|\mathbf{u}(L, \cdot) - \mathbf{u}_1^{2n}(L, \cdot)\|_2 + \|\mathbf{u}(0, \cdot) - \mathbf{u}_2^{2n}(0, \cdot)\|_2 \leq R^n (\|\mathbf{u}(L, \cdot) - \mathbf{u}_1^0(L, \cdot)\|_2 + \|\mathbf{u}(0, \cdot) - \mathbf{u}_2^0(0, \cdot)\|_2), \quad (4.5)$$

and the convergence factor is

$$R_{td} = \frac{\sqrt{L\eta + 2} - \sqrt{L\eta}}{\sqrt{L\eta + 2} + \sqrt{L\eta}} e^{-\sqrt{L\eta}\sqrt{L\eta+2}} < 1. \quad (4.6)$$

Proof. This result follows like in the time harmonic case, simply replacing $i\omega$ by $\sqrt{\eta}$. The convergence factor in Fourier is

$$\rho(|\mathbf{k}|) = \left| \frac{\sqrt{|\mathbf{k}|^2 + \eta} - \eta}{\sqrt{|\mathbf{k}|^2 + \eta} + \eta} e^{-\sqrt{|\mathbf{k}|^2 + \eta}L} \right|,$$

and the method thus converges for all Fourier modes. To conclude the proof, it suffices to take the maximum of the convergence factor over $|\mathbf{k}|$. \square

The preceding theorem shows that the classical Schwarz algorithm with Dirichlet transmission conditions applied to the time-discretized Maxwell's equations is convergent for all frequencies $|\mathbf{k}|$, and that the overlap is not necessary to ensure convergence. The classical Schwarz algorithm corresponds to a simple optimized Schwarz algorithm for the associated positive definite Helmholtz equation (4.2). With this equivalence, Lemma 3.5, Remark 2, Proposition 3.7 and all the cases in subsection 3.5 hold unchanged upon replacing $i\omega$ by $\sqrt{\eta}$, so we do not restate these results here. We show however in Table 4.1 the asymptotically optimal parameters to use in the time domain case, since they are fundamentally different from the time harmonic case and real, $s = p \in \mathbb{R}$ and $s_l = p_l \in \mathbb{R}$, $l = 1, 2$.

It is interesting to note a relationship of the optimized parameters for the time domain case with the one for Cauchy-Riemann, see [11]: Case 2 and 4 are identical, since the corresponding convergence rates in the two cases are the same, while for Case 1, 3 and 5 there is a small difference in the constants, which is due to the additional low frequency term in the Maxwell case. The difference appears to be systematic, the convergence factor of the Maxwell case is obtained from the convergence factor of the Cauchy-Riemann case by replacing h by $2h$, while for the optimized parameters one has to multiply by 2 in addition to the replacement of h by $2h$.

5. Numerical Experiments. We discretize the equations using a finite volume method, on a uniform mesh with mesh parameter h . In all comparisons that follow, we simulate directly the error equations, $f = 0$, and we use a random initial guess to ensure that all the frequency components are present in the iteration.

We first show the two dimensional problem of transverse electric waves, since this allows us to compute with finer mesh sizes and thus to illustrate our asymptotic results by numerical experiments. We then show also the full 3d case.

5.1. Two-dimensional case. We consider the transverse electric waves problem (TE) in the plane $(x, y, 0)$. There is no more dependence on z and the components E_3, H_1, H_2 are identically zero. The problem obtained is formally identical to the three-dimensional case (2.3), if $\mathbf{u} = (E_1, E_2, H_3)^t$, and the matrix $N_{\mathbf{v}}$ becomes

$$N_{\mathbf{v}} = \begin{pmatrix} -v_y \\ v_x \end{pmatrix},$$

and the matrices G_x, G_y and $G_{\mathbf{v}}$ are

$$G_x = \begin{pmatrix} N_{\mathbf{e}_x} \\ N_{\mathbf{e}_x}^t \end{pmatrix}, \quad G_y = \begin{pmatrix} N_{\mathbf{e}_y} \\ N_{\mathbf{e}_y}^t \end{pmatrix} \quad \text{and} \quad G_{\mathbf{v}} = \begin{pmatrix} N_{\mathbf{v}} \\ N_{\mathbf{v}}^t \end{pmatrix}.$$

All the analytical results remain valid, we only need to replace $|\mathbf{k}|$ by $|k_y|$, and the corresponding quantities in the optimized parameters for both time-harmonic and time-discretized solutions. We solve Maxwell's equations on the unit square $\Omega = (0, 1)^2$, decomposed into the two subdomains $\Omega_1 = (0, \beta) \times (0, 1)$ and $\Omega_2 = (\alpha, 1) \times (0, 1)$, where $0 < \alpha \leq \beta < 1$, and therefore the overlap is $L = \beta - \alpha$, and we consider both decompositions with and without overlap.

In the time-harmonic case, the frequency $\omega = 2\pi$ is chosen such that the rule of thumb of 10 points per wavelength is not violated. Table 5.1 shows the iteration count for all Schwarz algorithms we considered, in the overlapping and non-overlapping case. The results are presented in the form $it_S(it_{GM})$, where it_S denotes the iteration number for the iterative version of the algorithm and it_{GM} the iteration number for the accelerated version using GMRES.

In Figure 5.1 we show the results we obtained in a graph, together with the expected asymptotics. Both on the left in the overlapping case and on the right in the non-overlapping one, the asymptotics agree quite well, except for the classical case with overlap, where the algorithm performs better than predicted by the asymptotic analysis. In the case of the Cauchy-Riemann equations, see [14], we analyzed such a discrepancy further and showed that certain discretizations of the hyperbolic system can introduce higher order terms in the discretized transmission conditions, which can improve the convergence behavior, as we observe it here.

For the time discretized Maxwell's equations we choose $\eta = 1$. Table 5.2 shows the iteration count for all Schwarz algorithms we considered, in the overlapping and non-

| | with overlap, $L = h$ | | | | without overlap, $L = 0$ | | | |
|--------|-----------------------|--------|--------|--------|--------------------------|--------|--------|--------|
| h | 1/16 | 1/32 | 1/64 | 1/128 | 1/16 | 1/32 | 1/64 | 1/128 |
| Case 1 | 18(17) | 27(21) | 46(27) | 71(33) | -(48) | -(73) | -(100) | -(138) |
| Case 2 | 16(13) | 16(14) | 17(15) | 20(17) | 28(22) | 36(26) | 50(34) | 68(40) |
| Case 3 | 10(12) | 12(13) | 14(14) | 16(17) | 31(20) | 40(23) | 56(25) | 81(28) |
| Case 4 | 17(13) | 17(14) | 20(16) | 22(18) | 26(20) | 28(24) | 33(28) | 38(30) |
| Case 5 | 10(12) | 12(13) | 14(15) | 17(18) | 41(24) | 53(26) | 63(30) | 73(32) |

TABLE 5.1

Number of iterations in the 2d time harmonic case to attain an error tolerance of $= 10^{-6}$ for different transmission conditions and different mesh sizes.

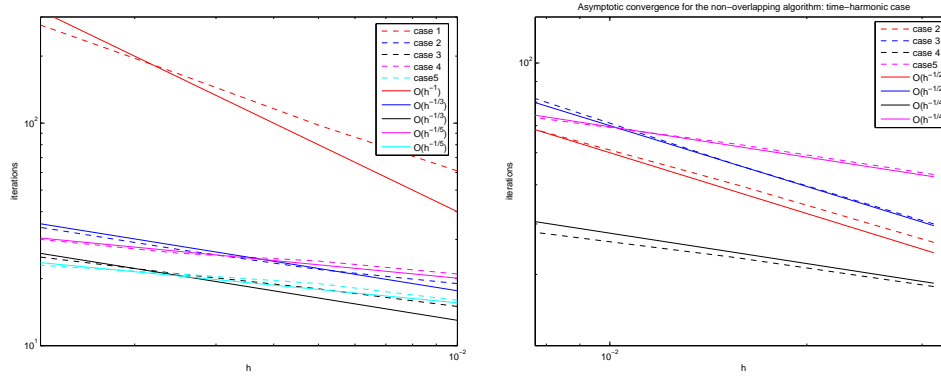


FIG. 5.1. Asymptotics for the overlapping (left) and non-overlapping (right) cases for the time harmonic equations.

overlapping case. We observe that the classical non-overlapping algorithm converges only very slowly, the need of optimized methods is evident here.

In Figure 5.2 we show the results we obtained in a graph, together with the expected asymptotics, and there is very good agreement.

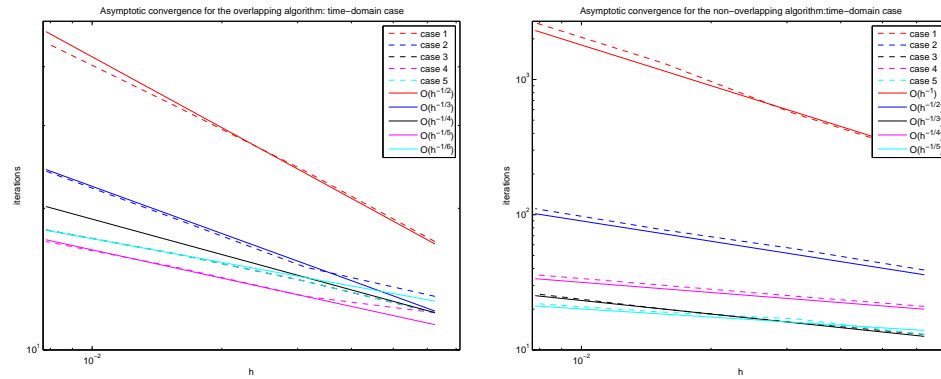


FIG. 5.2. Asymptotics for the overlapping (left) and non-overlapping (right) cases for the time discretized equations.

| | with overlap, $L = h$ | | | | without overlap, $L = 0$ | | | |
|--------|-----------------------|------|------|-------|--------------------------|------|------|-------|
| h | 1/16 | 1/32 | 1/64 | 1/128 | 1/16 | 1/32 | 1/64 | 1/128 |
| Case 1 | 17 | 24 | 33 | 45 | 280 | 559 | 1310 | 2630 |
| Case 2 | 13 | 15 | 19 | 24 | 39 | 56 | 77 | 111 |
| Case 3 | 12 | 14 | 16 | 18 | 13 | 16 | 20 | 26 |
| Case 4 | 12 | 13 | 15 | 17 | 21 | 25 | 30 | 36 |
| Case 5 | 12 | 14 | 16 | 18 | 13 | 17 | 19 | 22 |

TABLE 5.2

Number of iterations in the 2d time discretized case to attain an error tolerance of 10^{-6} for different transmission conditions and different mesh sizes.

| | with overlap, $L = h$ | | | without overlap, $L = 0$ | | |
|--------|-----------------------|--------|--------|--------------------------|--------|---------|
| h | 1/8 | 1/16 | 1/30 | 1/8 | 1/16 | 1/30 |
| Case 1 | 19(13) | 29(17) | 46(22) | -(93) | -(140) | -(202) |
| Case 2 | 14(12) | 19(14) | 23(16) | 48(29) | 69(36) | 98(48) |
| Case 3 | 16(12) | 18(14) | 21(16) | 65(35) | 80(42) | 166(55) |
| Case 4 | 15(13) | 19(15) | 22(17) | 38(28) | 60(33) | 104(39) |
| Case 5 | 16(13) | 18(14) | 21(16) | 70(36) | 80(42) | 176(55) |

TABLE 5.3

Number of iterations in the 3d time harmonic case to attain an error level of 10^{-6} for different transmission conditions and different mesh sizes.

5.2. Three-dimensional case. We solve now Maxwell's equations on the unit cube $\Omega = (0, 1)^3$. We decompose the domain into two subdomains $\Omega_1 = (0, \beta) \times (0, 1)^2$ and $\Omega_2 = (\alpha, 1) \times (0, 1)^2$, with $0 < \alpha \leq \beta < 1$, and $L = \beta - \alpha$ as before. In the time-harmonic case, we chose the frequency $\omega = 2\pi/3$ to satisfy the rule of thumb of 10 points per wavelength. Table 5.3 shows the iteration count for all Schwarz algorithms we considered, both in the overlapping and non-overlapping case.

The results for the time discretized Maxwell's equations where $\eta = 1$ are shown in Table 5.4.

6. Conclusions. We have shown that for Maxwell's equations, a classical Schwarz algorithm using characteristic Dirichlet transmission conditions between subdomains is equivalent to an optimized Schwarz method applied to a Helmholtz equation, with a low frequency approximation of the optimal transmission conditions. This equivalence shows that the classical Schwarz algorithm with characteristic Dirichlet conditions for Maxwell's equations is convergent, even without overlap. This equivalence allowed us to develop easily an entire hierarchy of optimized Schwarz methods with better transmission conditions than the characteristic ones for Maxwell's equations. We illustrated with numerical experiments that the new algorithms converge much more rapidly than the classical ones.

The equivalence between systems and scalar equations has already been instrumental for the development of optimized Schwarz algorithms for the Cauchy-Riemann equations, and will almost certainly play an important role for other cases. For example, it was already observed in [14] that for Euler's equation, the classical Schwarz algorithm with characteristic information exchange at the interfaces is convergent, even without overlap.

| | with overlap, $L = h$ | | | without overlap, $L = 0$ | | |
|--------|-----------------------|------|------|--------------------------|------|------|
| h | 1/8 | 1/16 | 1/30 | 1/8 | 1/16 | 1/30 |
| Case 1 | 14 | 18 | 25 | 246 | 467 | 859 |
| Case 2 | 13 | 18 | 22 | 46 | 65 | 87 |
| Case 3 | 12 | 15 | 17 | 47 | 59 | 73 |
| Case 4 | 14 | 17 | 19 | 48 | 57 | 66 |
| Case 5 | 12 | 14 | 16 | 46 | 53 | 60 |

TABLE 5.4

Number of iterations in the 3d time discretized case to attain an error level of 10^{-6} for different transmission conditions and different mesh sizes.

- [1] A. Alonso-Rodriguez and L. Gerardo-Giorda. New non-overlapping domain decomposition methods for the time-harmonic maxwell system. *SIAM J. Sci. Comp.*, 28(1):102–122, 2006.
- [2] T. F. Chan and T. P. Mathew. Domain decomposition algorithms. In *Acta Numerica 1994*, pages 61–143. Cambridge University Press, 1994.
- [3] P. Charton, F. Nataf, and F. Rogier. Méthode de décomposition de domaine pour l'équation d'advection-diffusion. *C. R. Acad. Sci.*, 313(9):623–626, 1991.
- [4] P. Chevalier and F. Nataf. Symmetrized method with optimized second-order conditions for the Helmholtz equation. In *Domain decomposition methods, 10 (Boulder, CO, 1997)*, pages 400–407. Amer. Math. Soc., Providence, RI, 1998.
- [5] S. Clerc. Non-overlapping Schwarz method for systems of first order equations. *Cont. Math.*, 218:408–416, 1998.
- [6] P. Collino, G. Delbue, P. Joly, and A. Piacentini. A new interface condition in the non-overlapping domain decomposition. *Comput. Methods Appl. Mech. Engrg.*, 148:195–207, 1997.
- [7] Q. Deng. An analysis for a nonoverlapping domain decomposition iterative procedure. *SIAM J. Sci. Comput.*, 18:1517–1525, 1997.
- [8] B. Després. Décomposition de domaine et problème de Helmholtz. *C.R. Acad. Sci. Paris*, 1(6):313–316, 1990.
- [9] B. Després. Domain decomposition method and the Helmholtz problem.II. In *Second International Conference on Mathematical and Numerical Aspects of Wave Propagation (Newark, DE, 1993)*, pages 197–206. Philadelphia, PA, 1993. SIAM.
- [10] B. Després, P. Joly, and J. E. Roberts. A domain decomposition method for the harmonic Maxwell equations. In *Iterative methods in linear algebra (Brussels, 1991)*, pages 475–484. Amsterdam, 1992. North-Holland.
- [11] V. Dolean and M. J. Gander. Why classical Schwarz methods applied to hyperbolic systems converge even without overlap. In *Seventeenth International Conference on Domain Decomposition Methods*, 2007.
- [12] V. Dolean and S. Lanteri. An implicate finite volume time-domain method on unstructured meshes for Maxwell equations in three dimensions. Technical Report 5767, INRIA, 2005.
- [13] V. Dolean, S. Lanteri, and F. Nataf. Construction of interface conditions for solving compressible Euler equations by non-overlapping domain decomposition methods. *Int. J. Numer. Meth. Fluids*, 40:1485–1492, 2002.
- [14] V. Dolean, S. Lanteri, and F. Nataf. Convergence analysis of a Schwarz type domain decomposition method for the solution of the Euler equations. *Appl. Num. Math.*, 49:153–186, 2004.
- [15] B. Engquist and H.-K. Zhao. Absorbing boundary conditions for domain decomposition. *Appl. Numer. Math.*, 27(4):341–365, 1998.
- [16] E. Faccioli, F. Maggio, a. Quarteroni, and A. Tagliani. Spectral domain decomposition methods for the solution of acoustic and elastic wave propagation. *Geophysics*, 61:1160–1174, 1996.
- [17] E. Faccioli, F. Maggio, A. Quarteroni, and A. Tagliani. 2d and 3d elastic wave propagation by pseudo-spectral domain decomposition method. *Journal of Seismology*, 1:237–251, 1997.
- [18] M. J. Gander. Optimized Schwarz methods. *SIAM J. Numer. Anal.*, 44(2):699–731, 2006.
- [19] M. J. Gander and L. Halpern. Méthodes de relaxation d'ondes pour l'équation de la chaleur en dimension 1. *C.R. Acad. Sci. Paris, Série I*, 336(6):519–524, 2003.
- [20] M. J. Gander, L. Halpern, and F. Magoulès. An Optimized Schwarz Method with two-sided Robin transmission conditions for the Helmholtz Equation. *Int. J. Numer. Meth. Fluids*,

2006. in press.
- [21] M. J. Gander, L. Halpern, and F. Nataf. Optimal Schwarz waveform relaxation for the one dimensional wave equation. *SIAM Journal of Numerical Analysis*, 41(5):1643–1681, 2003.
 - [22] M. J. Gander, F. Magoulès, and F. Nataf. Optimized Schwarz methods without overlap for the Helmholtz equation. *SIAM J. Sci. Comput.*, 24(1):38–60, 2002.
 - [23] T. Hagstrom, R. P. Tewarson, and A. Jazcilevich. Numerical experiments on a domain decomposition algorithm for nonlinear elliptic boundary value problems. *Appl. Math. Lett.*, 1(3), 1988.
 - [24] C. Japhet, F. Nataf, and F. Rogier. The optimized order 2 method. application to convection-diffusion problems. *Future Generation Computer Systems FUTURE*, 18, 2001.
 - [25] P.-L. Lions. On the Schwarz alternating method. III: a variant for nonoverlapping subdomains. In T. F. Chan, R. Glowinski, J. Périaux, and O. Widlund, editors, *Third International Symposium on Domain Decomposition Methods for Partial Differential Equations*, held in Houston, Texas, March 20-22, 1989, Philadelphia, PA, 1990. SIAM.
 - [26] F. Nataf and F. Rogier. Factorization of the convection-diffusion operator and the Schwarz algorithm. *M³AS*, 5(1):67–93, 1995.
 - [27] J.-C. Nédélec. *Acoustic and electromagnetic equations. Integral representations for harmonic problems*. Applied Mathematical Sciences, 144. Springer Verlag, 2001.
 - [28] A. Quarteroni. Domain decomposition methods for systems of conservation laws: spectral collocation approximation. *SIAM J. Sci. Stat. Comput.*, 11:1029–1052, 1990.
 - [29] A. Quarteroni and L. Stolic. Homogeneous and heterogeneous domain decomposition methods for compressible flow at high Reynolds numbers. Technical Report 33, CRS4, 1996.
 - [30] A. Quarteroni and A. Valli. *Domain Decomposition Methods for Partial Differential Equations*. Oxford Science Publications, 1999.
 - [31] D. Serre. *Systems of conservation laws*. Hyperbolicity, entropies, shock waves. Cambridge University Press, 1999.
 - [32] B. F. Smith, P. E. Bjørstad, and W. Gropp. *Domain Decomposition: Parallel Multilevel Methods for Elliptic Partial Differential Equations*. Cambridge University Press, 1996.
 - [33] I. Sofronov. Nonreflecting inflow and outflow in a wind tunnel for transonic time-accurate simulation. *J. Math. Anal. Appl.*, 221(1) 92, 1998.
 - [34] H. Sun and W.-P. Tang. An overdetermined Schwarz alternating method. *SIAM Journal on Scientific Computing*, 17(4):884–905, Jul. 1996.
 - [35] W. P. Tang. Generalized Schwarz splittings. *SIAM J. Sci. Stat. Comp.*, 13(2):573–595, 1992.
 - [36] A. Toselli. Overlapping Schwarz methods for Maxwell’s equations in three dimensions. *Numer. Math.*, 86(4):733–752, 2000.
 - [37] A. Toselli and O. Widlund. *Domain Decomposition Methods - Algorithms and Theory*, volume 34 of *Springer Series in Computational Mathematics*. Springer, 2004.
 - [38] J. Xu. Iterative methods by space decomposition and subspace correction. *SIAM Review*, 34(4):581–613, December 1992.
 - [39] J. Xu and J. Zou. Some nonoverlapping domain decomposition methods. *SIAM Review*, 40:857–914, 1998.

Asymptotic convergence for the overlapping algorithm: time-harmonic case

